Assessing geothermal risk prior to drilling

Alexandros Daniilidis[1], Leon Doddema[1] and Rien Herber[1]

[1] University of Groningen, Nijenborgh 4, 9747 AG Groningen, The Netherlands

a.daniilidis@rug.nl

Keywords: direct use, 3D numerical model, uncertainty, risk assessment, Rotliegend.

ABSTRACT

The planning phase of geothermal projects involves diverse levels of uncertainty. Consequently, risk remains high prior to exploration drilling. Generating a qualitative risk matrix, supported by numerical results can aid the decision-making process during the planning phase of a geothermal installation.

A discrete parameter analysis can be employed to rank the relative influence of these uncertainties. In this setting, uncertainty is classified in three main categories, namely: initial subsurface conditions (pressure, gas saturation), geological and geophysical properties (permeability and fault seal) and lastly operational parameters (flow rate and re-injection temperature). By populating the uncertainty classes with discrete values and simulating all combinations, a qualitative and quantitative risk assessment can be performed.

Using the case study of the envisioned Groningen geothermal doublet, we present a workflow that integrates seismic, petrophysical and reservoir data. The generated risk matrix identifies pressure depletion as a major project risk. Furthermore, power generation can be maintained beyond 60 years, while similar power output can be achieved with different combinations of flow rate and re-injection temperature.

1. INTRODUCTION

In the North Netherlands, a geothermal project is on the agenda of the municipality of Groningen. The Permian Rotliegend sandstone is considered as a target aquifer. The sandstone holds the nearby Groningen gas field and is a proven good quality reservoir. The top Rotliegend Slochteren sandstone in the license area lies at circa 3,400m with an average thickness of 250m.

Although there is good seismic data coverage in the greater area, some uncertainties remain irreducible before drilling. Previous work on uncertainties related to geothermal production has considered a breadth of parameters (Vogt et al., 2010; Mottaghy et al., 2011; Vogt et al., 2013; Saeid et al., 2015; van Wees et al., 2012).

Two unique conditions are encountered in our research area. Firstly, gas production from the Groningen field has resulted in pressure depletion inside the ROSL formation. The extent and magnitude of this pressure depletion cannot be estimated accurately with the available data. Secondly, some amount of dissolved gas is expected to be present in the area considered for geothermal development. These two conditions further complicate the uncertainty analysis.

This work focuses on assessing and prioritizing the geothermal risk. Three levels of uncertainty are used:

Initial aquifer state (pressure depletion and gas saturation)

Reservoir (rock and fault permeability)

Operational (flow rate and re- injection temperature)

A discrete parameter analysis is used to consider all possible parameter combinations. Additionally the reservoir model is based on 3D seismic data interpretation.

2. BACKGROUND AND GEOLOGICAL SETTING

The shallower parts of the Slochteren sandstone that constitute the Groningen High (2,800m to 3,000m (Grötsch et al., 2011)) are gas bearing. As a result seismic surveys and wells are widespread in the area (de Jager and Geluk, 2007; Grötsch et al., 2011)

Though extensively explored for gas, the Rotliegend sandstone is not a common geothermal target in the Netherlands yet. A single project in the Koekoekspolder region (North Netherlands region) encountered anhydrite cementation (Henares et al., 2014). This resulted in lower than predicted values of permeabilities and net-to-gross.

The Groningen geothermal concession lies in the Northwest of the city, in the Lauwerszee Trough. Despite the many records of pressure (Verweij et al., 2011) and temperature gradients (Bonté et al., 2012) in the greater area, the gas production of the Groningen field has caused pressure

depletion that could extend beyond the field itself (Breunese and van Thienen-Visser, 2014).

Therefore, the pressure in the concession area could range from hydrostatic levels down to the current pressure level of the gas field. Additionally, the underlying Westphalian coal source rock and the proximity to the Groningen and smaller gas fields suggest that gas could also be present in the concession.

Uncertainty regarding geological conditions relates to reservoir characteristics, but also the behaviour of faults as conduits or barriers to flow. Faults that compartmentalize Rotliegend reservoirs are known to be present in the area (Ligtenberg et al., 2011; Van Hulten, 2010). Project operating conditions are not strictly defined and therefore add to the uncertainty.

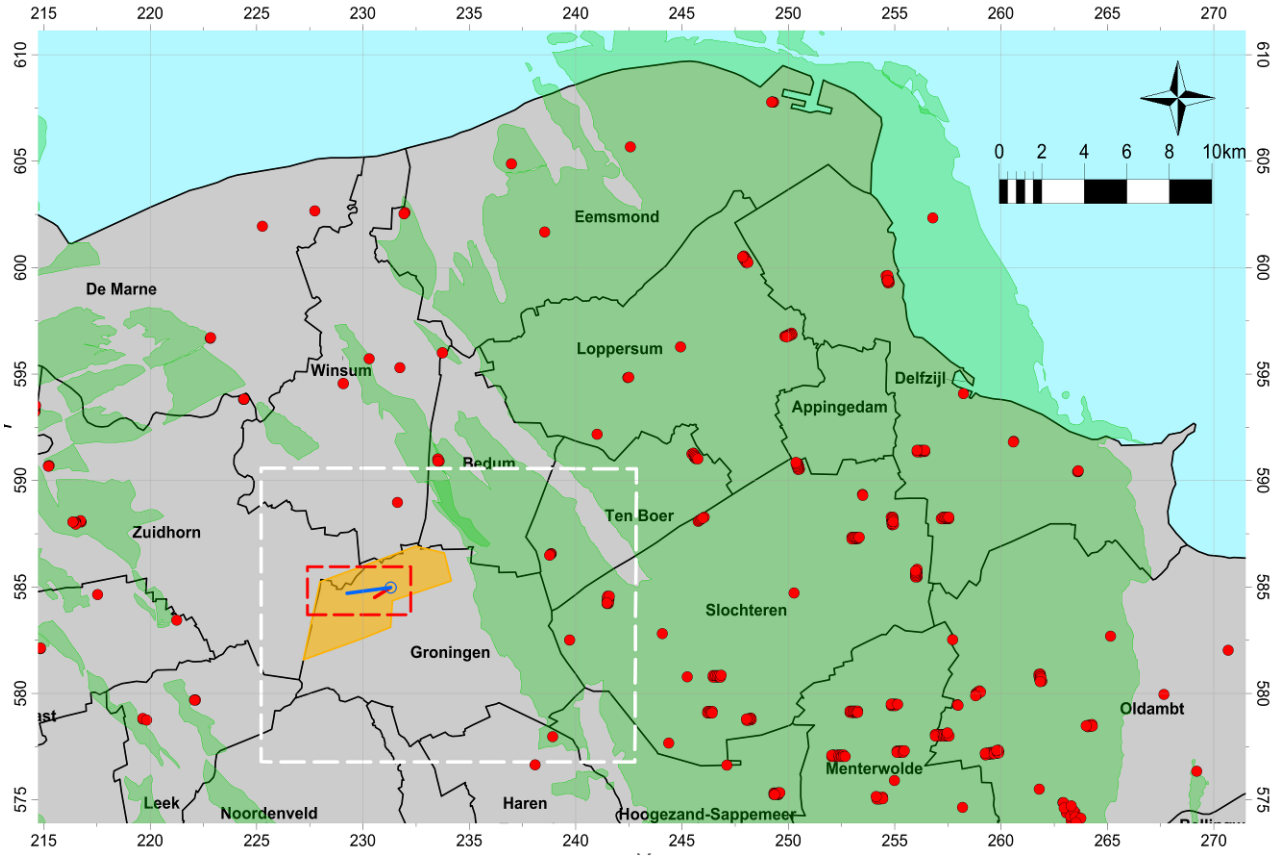

Figure 1. Area of interest in the north of the Netherlands. Gas fields are plotted in green, the orange surface indicates the geothermal license, white rectangle indicates the extent of the interpreted 3D seismic cube and the red dashed rectangle outlines the reservoir model. Proposed well trajectories are indicated with blue (injector) and red (producer) lines. Red dots mark the location of existing gas wells, while aggregated dots indicate the presence of a cluster. Map coordinates are in RD-new.

3. METHODS

A streamlined workflow from seismic data to reservoir parameter assessment is used in this analysis. Seismic interpretation was carried out in Petrel (Schlumberger, 2012). The PetraSim (Rockware, 2014) software in combination with PyTOUGH (Croucher, 2014; Florian Wellmann et al., 2012) was used for the simulations. The EWASG (Equation of State for Water, Salt and Gas) was used to accommodate two phase flow of water, salt and CH4 in the reservoir (Battistelli et al., 1997).

3.1 Geological and petrophysical data

3D Pre-Stack Depth Migrated (PSDM) seismic data provided by NAM was used for interpreting the main stratigraphic units. The data cube has dimensions of 17.5km x 13.7km x 4km (N-S, E-W, depth). The interpreted fault and horizon surfaces were the input for the structural framework and geological modelling.

Petrophysical data were provided for gross thickness, net sand, net-to-gross ratio, porosity and permeability (P90-P50-P10) per layer and per well (van Leeuwen et al., 2014). A total of 8 wells were used for the petrophysical data (EKL-01, NRD-01, PSP-01, ROD-101, SSM-01, SSM-02, SAU-01, TBR-04). The data were re-aggregated using a double weighting factor for the SAU-01 well that is closest to the concession. Vertical permeability values were assigned as on order of magnitude lower than the respective horizontal permeability (Carlson, 2003), thus accounting for angled well to reservoir contacts.

3.2 3D reservoir model

The domain of the reservoir has dimensions of 4.9km x 2.3km (E-W, N-S) and extends between 2.9km and 3.9km depth. The cell dimensions are 50m x 50m on the horizontal plane. The vertical dimension varies per layer and ranges between 24m and 59m. The resulting cell count is 47,520.

The two major faults included in the reservoir model are mapped with the same grid resolution as the matrix rock.

The initial reservoir state is computed using a geothermal gradient of 31.3°C/km (Bonté et al., 2012) and a pressure gradient of 0.1bar/m for the reservoir overburden. The

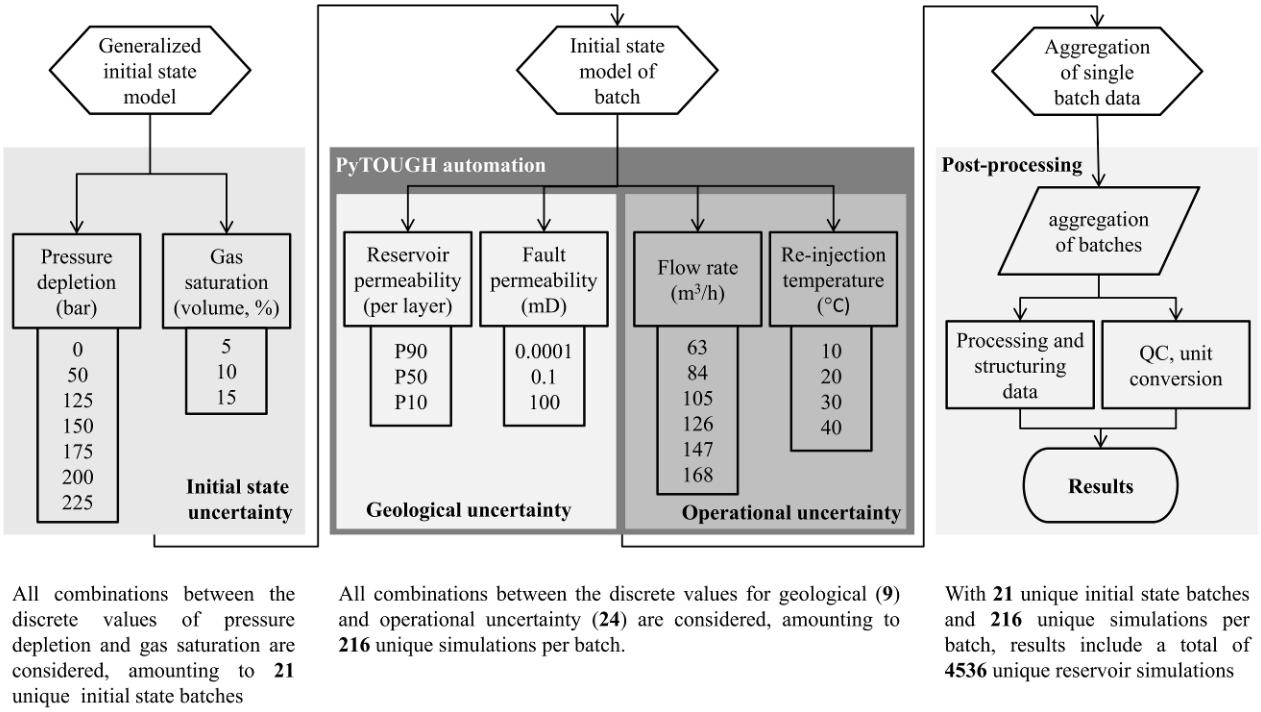

Figure 2. Discrete steps followed for the reservoir simulation workflow. Due the amount of data produced by the simulations, only the results on the injector and producer cells were stored and are included in the results.

reservoir pressure further uses scenarios ranging from 0 to 225 bar depletion. Salt concentration in the reservoir is in the order of 250,000ppm (Bolourinejad and Herber, 2015).

Based on the fault interpretation, the wells target the largest un-faulted block in the concession. Additionally well design considers the possibility to encounter a depleted reservoir by using as much as possible a vertical producer trajectory. The distance between the wells is 1,250m at reservoir depth.

3.1 PyTOUGH automating and uncertainty

The initial state models consist of all combinations of values between pressure depletion and gas saturation (21 versions). Each initial state model is further differentiated using a unique value combination of the other uncertainty classes. The total number of unique full reservoir simulation runs is 4536 (Figure 2).

The initial state models were prepared and inspected in PetraSim. For each initial state version, the other uncertainty parameters where automated using PyTOUGH scripts. Flow rate level for both wells was kept constant throughout the 100 years of simulation time.

4. RESULTS

Results are categorized by five model outputs: Thermal power (MW), Δp producer-injector (bar), Δp producer-hydrostatic reservoir (bar), Producer temperature (°C) and Gas to brine ratio (m^3/m^3). The influence of each uncertainty class to the aforementioned outputs is quantified and ranked.

4.1 Thermal power

Flow rate levels control the thermal power output of the doublet (Figure 3). Within the envelope of the flow rate, other parameters (pressure depletion, gas saturation) could introduce a variability of up to +/-1MW. Re-injection temperature levels remain important as the extracted power is always the difference between power output and input.

Fault permeability becomes important over time, as sealing faults reduce the affected reservoir volume, leading to an earlier drop in power. This temporal effect becomes more pronounced with higher flow rates..

The mean power per parameter group and values is shown in Figure 4, highlighting input sensitivity. Mean values are partly dependent and therefore do not exhibit the full range of values as shown in Figure 3. Results show the highest spread in values being caused by flow rate. Within the spread, higher flow rates show a wider spread over time. Re-injection temperature appears to have a linear effect which becomes stronger with time. High permeable faults cause a smaller decrease in power over time, while sealing faults result in a significant decrease in power delivery. Other parameters only have minor effects to power output.

4.2 Δp producer - injector

At the same reservoir permeability high fault permeability faults results in lower pressure differences (Figure 5). However, differences between middle and low fault permeability are not so distinctive. In all cases the

differences caused by fault permeability become more pronounced over time.

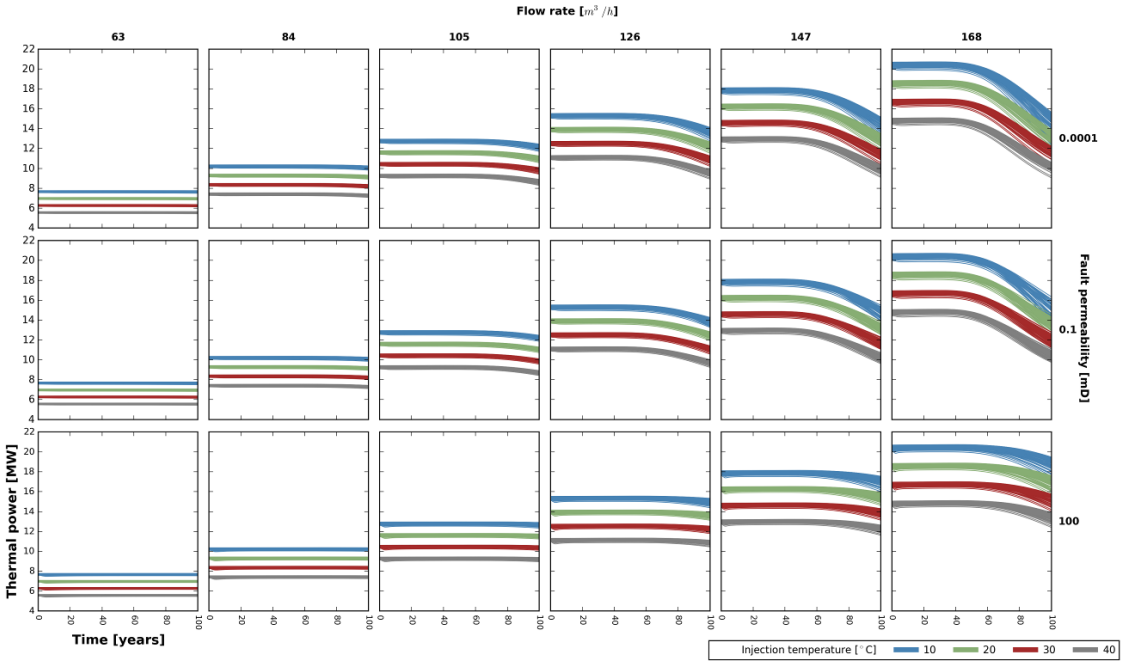

Figure 3. Thermal power output (MW) as a function of time, flow rate, fault permeability and injection temperature. "Spread" between the injection temperature effect increases with higher flow rates. Breakthrough occurs sooner (curves bend) with higher flow rates and sealing faults. Permeable faults extend the lifetime of the system.

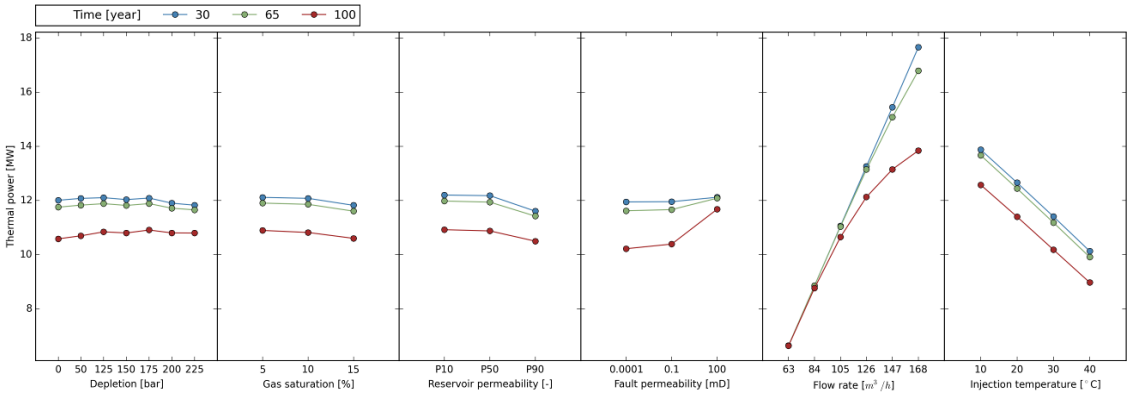

Figure 4. Mean values of thermal output (MW) for all uncertainty classes. The co-dependency of the variables causes the mean values presented to be different (lower) than the absolute values of the individual simulations in Figure 3.

Within the range defined by flow rate, reservoir permeability and the temporal effect of the faults, differentiation is caused by the remaining parameters (i.e. pressure depletion, gas saturation and injection temperature). Reservoir permeability is more influential than flow rate (Figure 6). Injection temperature has an increasing effect over time, but the impact reduces gradually with higher temperatures. Lastly, high fault permeability has a smaller impact to the well pressure difference than middle and low fault permeability.

4.3 Δp producer - hydrostatic reservoir

Possible pressure depletion in the aquifer has a strong effect on the doublet CoP (Coefficient of Performance) since it determines the power required to bring the water to surface. Using an average reservoir pressure of 360 bar (hydrostatic pressure level at average reservoir depth), the pressure difference between producer well and hydrostatic reservoir is computed (Figure 7). Absolute pressure values are controlled by the degree of pressure depletion caused by the gas production in the concession. Depletion levels seem to cause the larger spread of the graphs. The influence of the flow rate level is decreasing with higher depletion levels. High (P10) and medium (P50) reservoir permeability result in a smaller envelope with higher absolute pressure values and significant overlap between flow rate levels. Lastly, low (P90) reservoir permeability increases the pressure drop for the same flow rate.

The sensitivity of the pressure difference between the producer well and a hydrostatic reservoir is dominated by pressure depletion levels (Figure 8). Reservoir permeability is the second most influential factor. Higher flow rate levels have a stronger effect that is increasing over time.

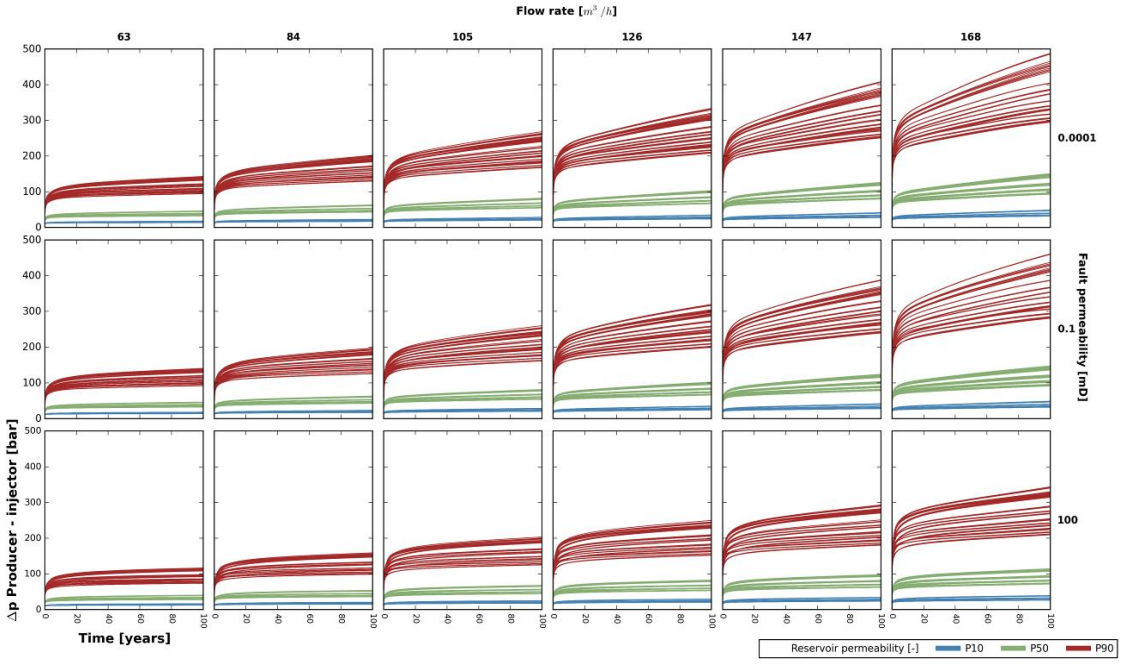

Figure 5. Pressure difference between producer and injector well as a function of time, flow rate, reservoir permeability and fault permeability.

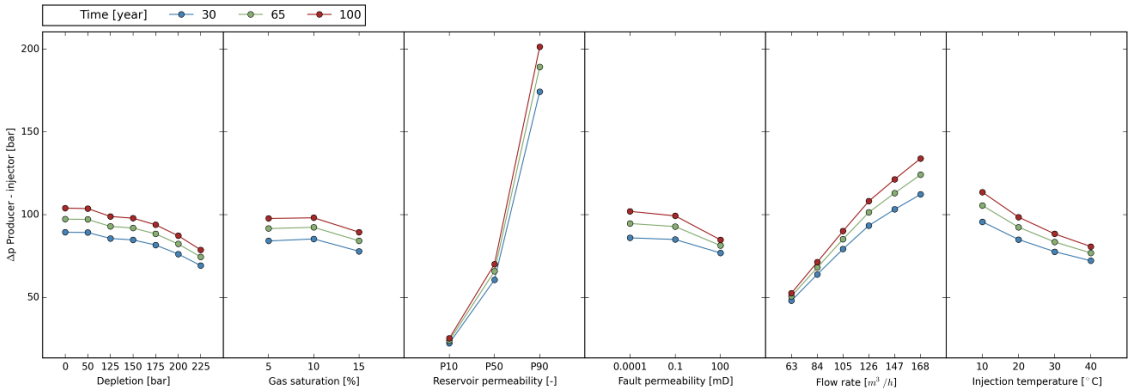

Figure 6. Mean values of pressure difference between injector and producer for all uncertainty classes and variables. Variable co-dependency causes the mean values presented to be different (lower) than the absolute values of the individual simulations in Figure 5.

4.4 Producer temperature

Producer well temperature is indicative of the depletion rate of the field. Temperature does not decrease before 45 years of production (Figure 9). Beyond 45 years the high flow rate simulations start to show a temperature decrease; this decrease however is in the order of 5°C around 60 years of production. The producer temperature remains higher than 100°C, even after 80 years of production.

Flow rate has the highest impact on producer temperature (Figure 10). Nonetheless, only the high flow rates cause a clear temperature drop after 65 years. Most other parameters have almost no effect on the producer temperature, with the exception of high fault permeability. The latter helps to keep producer temperature high, since the rock volume affected is larger. Gas saturation and injection temperature seem to have almost no effect even after 100 years of production.

4.5 Gas to brine ratio

All gas to brine ratio results exhibit a spike within the first 10 years of production (Figure 11). This can be attributed to the pressure front from the injector well reaching the producer and displacing the gas. Following this, gas levels stabilize earlier for lower and later for higher flow rates. For low initial gas saturation, minor amounts of gas are produced. For middle and high initial gas saturation there is a clear ordering with lower reservoir permeability leading to higher gas production. This is attributed to an increase in absolute gas permeability for low permeability values according to the Klinkenberg effect (Tanikawa and Shimamoto, 2009). With increasing reservoir permeability, gas is not displaced as effectively and smaller amounts are produced.

Even though initial gas saturation dominates the gas to brine ratio, all parameters seem to affect this (Figure 12). Pressure

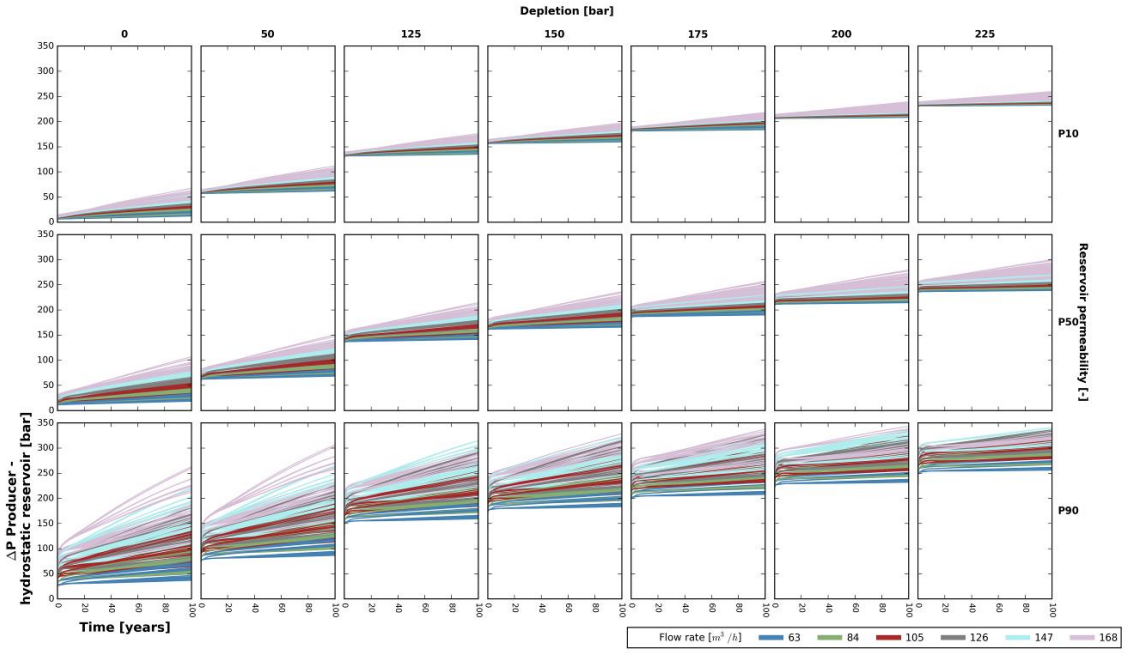

Figure 7. . Pressure difference between producer and hydrostatic reservoir pressure (no depletion). The pressure values represent the pumping pressure needed in the producer for the water to reach the surface. The lowest value in each subplot represents the equivalent depth at which the pump needs to be installed.

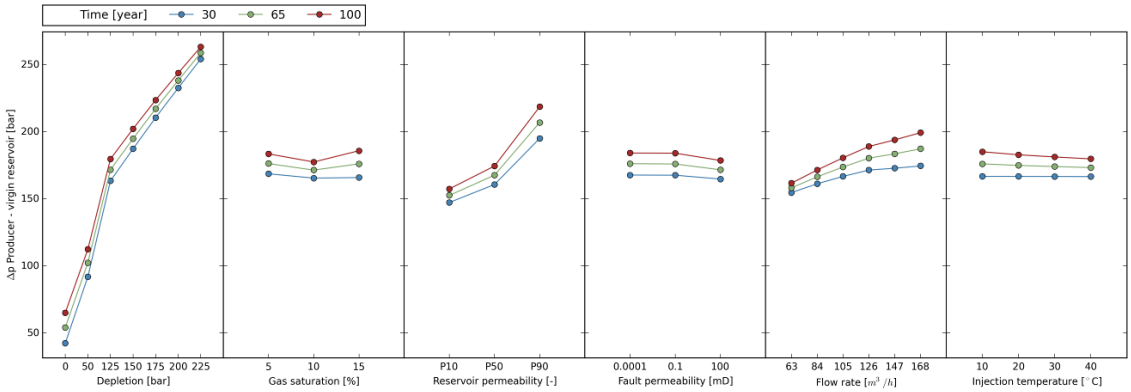

Figure 8. Mean values of Δp between producer and hydrostatic reservoir (360 bar) for all uncertainty classes. The pressure difference values in the graph represent the hydraulic head that a producer pump would need to overcome.

.

depletion is crucial since a given gas saturation at reservoir level results gas volume inside the reservoir and hence to standard conditions at surface. Therefore, no depletion results in higher gas volumes produced. Low reservoir permeability values (P90) result in larger gas volume production than medium (P50) and high reservoir permeability (P10). High reservoir permeability also leads to more gas production, though this effect is minimized over time. The positive effect of increasing flow rate is small and a plateau is observed above 126m^3/hr.

5. DISCUSSION

Initial state uncertainty mainly impacts the pressure difference between the well and the reservoir, as well as the amount of produced gas. Concretely, *pressure depletion* mostly influences the pressure difference between the producer well and a hypothetical undisturbed reservoir pressure level. As a result, pressure depletion controls the depth at which the production pump needs to be installed, which needs to be taken into account when the well trajectory is designed. This aspect was thus considered in the presented well placement in Groningen, also taking into account spatial restrictions formed by surface facilities, concession extent and internal reservoir architecture. Nonetheless, higher pressure drops could be computed with a finer mesh around the wells. Additionally if pressure depletion is present it could further progress during the production period (Van Wees et al., 2014), since gas production is still ongoing.

Gas saturation levels have a dominant effect on the produced gas to brine ratio. High gas to brine ratios could potentially yield additional income for a geothermal project (van Heekeren and Bakema, 2015). At the same time the technical feasibility of the pump installation and surface facilities could be complicated as a result (Frick et al., 2011; van Heekeren and Bakema, 2015).

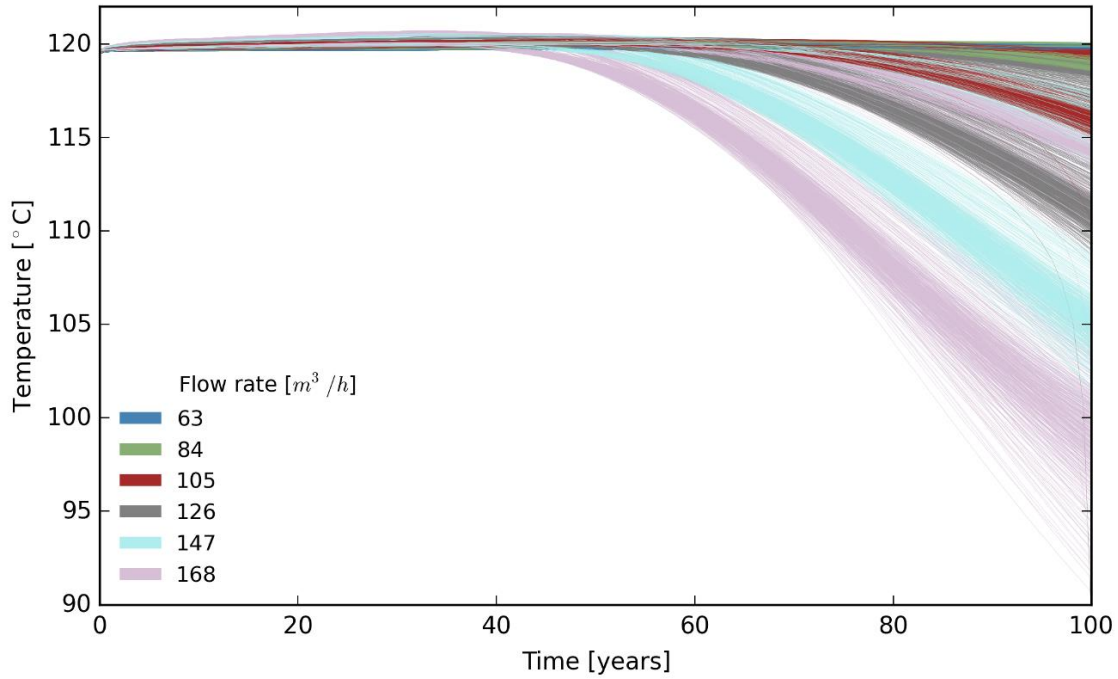

Figure 9 Producer well temperature data for all 4377 simulation scenarios. Temperature drops by 10% of the initial production temperature only after around 75 years of simulation. A drop in produced water is not observed in any case before 45 years of production. Breakthrough time is not a significant parameter for the operations design.

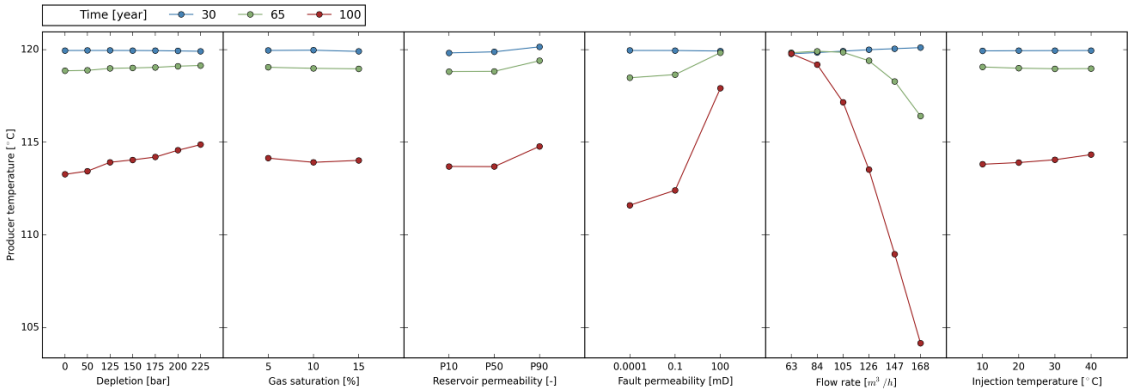

Figure 10. Mean values of producer temperature for all uncertainty classes

Geological uncertainty is more pertinent to pressure output and secondly to gas production and temperature output. *Reservoir permeability* governs the pressure difference between wells, thus determining the required pumping energy. Limitations related to low reservoir permeability could be overcome by hydraulic stimulation as demonstrated in Rotliegend sediments at the Groß Schönebeck field (Legarth et al., 2005; Zimmermann and Reinicke, 2010). Alternatively a hybrid system between the two versions of natural and stimulated reservoir (Blöcher et al., 2015), or more sophisticated well-reservoir coupling could be used.

Fault permeability has mostly temporal effects on well temperature and thermal power and smaller influence on the gas to brine ratio. Essentially presence and permeability of faults affect the fluid volume connected to the doublet. Sealing faults confine the reservoir volume and alter heat extraction and gas production levels. This highlights the importance of 3D geometric reservoir modelling as such aspects would remain undetected through a simplified 2D model.

Operational uncertainty influences all outputs except gas to brine ration levels. *Flow rate* largely defines thermal power, producer temperature and doublet pressure difference. Nonetheless there is some degree of freedom that allows for a trade-off: the same power output can be achieved through more than one combination of flow rate and injection temperature. Flow rate is still important for pressure difference levels between producer and hydrostatic reservoir. This effect however could be underestimated due to mesh resolution around the wells and the difference between dynamic and static fluid level (Frick et al., 2011).

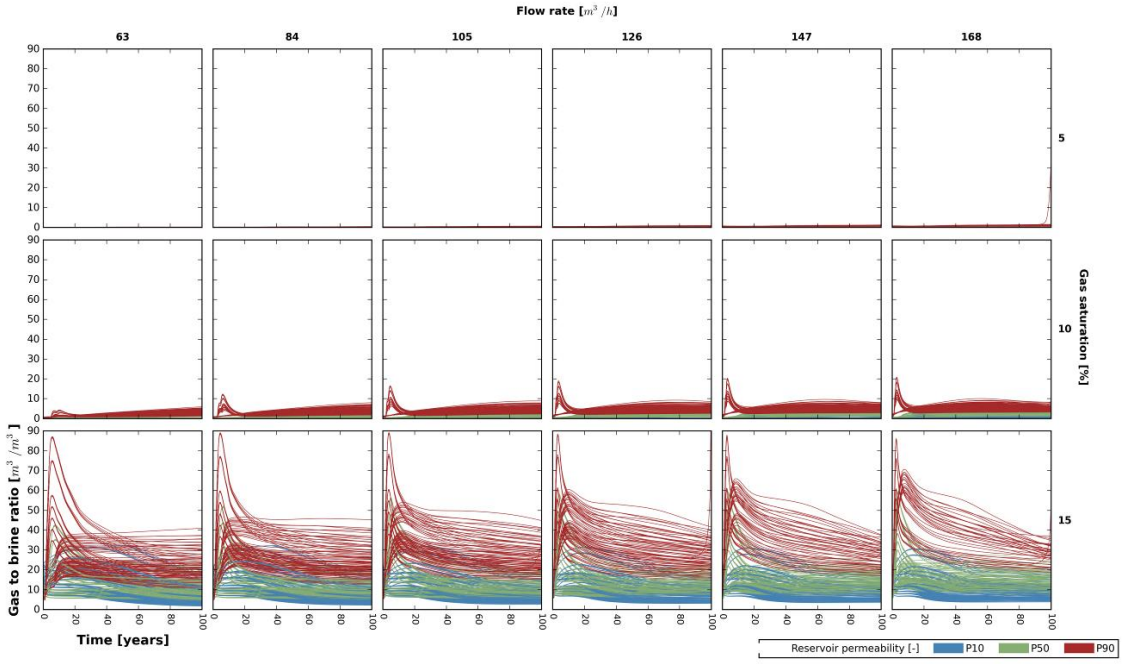

Figure 11. Amount of gas m3 produced for every m3 of water at surface conditions. Gas saturation has a major effect and more gas is produced at higher initial saturation.

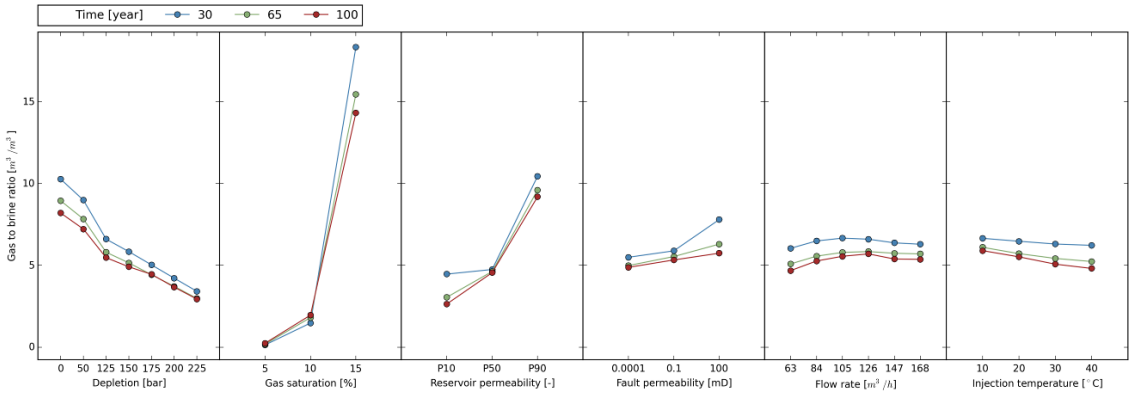

Figure 12. Mean values for gas to brine ratio for all uncertainty classes.

Re-injection temperature controls the amount of extracted heat from the reservoir and the power output. Therefore, this aspect should be really considered when deciding the doublet dimensioning. Pressure difference between the wells is moderately affected by re-injection temperature and mostly relates to density and viscosity difference caused by temperature (Francke and Thorade, 2010).

The method used enables the production of a comprehensive risk matrix (Table 1) with regard to the uncertainty levels of initial state, geological and operational parameters. The parameter co-dependency highlights the relative importance of each considered input. The matrix can therefore be used to better direct future efforts prior to drilling the exploration well. The use of 3D field geometry and 3D numerical simulations supports both quantitative and qualitative insights and can lead to more successful implementation of direct use geothermal projects.

Early decisions on doublet sizing or engineering requirements and restrictions could reduce the number of simualtions needed. In the absence of data availability, a careful selection of parameters and ranges could still yield useful results through the proposed methodology and widen its applicability.

6. CONCLUSION

The employed methodology results in a comprehensive reservoir risk assessment of a geothermal direct use installation. Three levels of uncertainty are included in the discrete parameter analysis, namely initial state, geological and operational uncertainty. The analysis is based on a 3D geological model and is carried out through an ensemble of 4536 unique numerical 3D reservoir simulations covering a production period of 100 years. All possible combinations of the discrete parameters are considered. The relative effect of each parameter class is extracted by means of a sensitivity analysis. A risk assessment matrix provides a qualitative overview, while the wealth of generated data deliver quantitative output ranges. While the methodology is transferable to other geothermal fields, the numerical results are restricted to the Groningen concession.

Table 1. Risk assemsent overview through the effect of uncertainty parameters to simulation output.

Uncertainty parameter	Output impact: Thermal power [MW]	Δp producer - injector [bar]	Δp producer - hydrostatic reservoir [bar]	Producer temperature [°C]	Gas to brine ratio [m^3/m^3]
Depletion [bar]	low	low	high	low	medium
Gas saturation [%]	low	low	low	low	high
Reservoir permeability [mD]	low	high	medium	low	medium
Fault permeability [mD]	low (temporal)	low	low	medium (temporal)	medium-low
Flow rate [m^3/h]	high	high	medium	high	low
Injection temperature [°C]	medium	medium	low	low	low

Making use of available data and uncertainty ranges with the methodology, we conclude that the thermal energy in the envisioned Groningen geothermal doublet (Rotliegend reservoir) can be sustained beyond 60 years (5°C temperature drop) under all simulations.

Regarding initial state uncertainty, pressure depletion can significantly affect the production pump installation depth. A pressure head of up to 325 bar could be required by the pump, resulting in major technical challenges. Therefore, reservoir pressure depletion is a major risk for geothermal projects. Reservoir gas saturation levels control the amount of gas that might be co-produced. Volumes of up to 90 m^3 of methane per m^3 of produced brine can be expected for a gas saturation of 15%.

Pressure difference within the reservoir is controlled by reservoir permeability. Low permeability (P90) can generate pressure differences up to 500 bar, while medium permeability (P50) only reaches differences up to 150 bar. Fault permeability, the second geological uncertainty parameter, affects the produced water temperature. Sealing faults start to affect the produced temperature after 60 years of simulation time.

Operational uncertainty parameters present mutual trade-offs As a result, the same power output can be achieved with more than one flow rate and re-injection temperature combination. Flow rate impacts both pressure and the thermal power outputs significantly. The Groningen geothermal doublet can produce power in excess of 21 MW with a Δp ranging between 50bar and 500bar (controlled by reservoir permeability). Additionally, injection temperature impacts power output and pressure. For the same flow rate up to 5 MW more can be extracted by reducing the injection temperature from 40°C to 10°C.

REFERENCES

Battistelli, A., Calore, C., Pruess, K., 1997. The simulator TOUGH2/EWASG for modelling geothermal reservoirs with brines and non-condensible gas. Geothermics 26, 437-464.

Blöcher, G., Cacace, M., Reinsch, T., Watanabe, N., 2015. Evaluation of three exploitation concepts for a deep geothermal system in the North German Basin. Computers & Geosciences 82, 120-129.

Bolourinejad, P., Herber, R., 2015. Experimental investigation of porosity and permeability variations in reservoirs and caprock following co-injection of sulfur dioxide and hydrogen sulfide with carbon dioxide. Journal of Petroleum Science and Engineering 129, 137-144.

Bonté, D., Van Wees, J.D., Verweij, J.M., 2012. Subsurface temperature of the onshore Netherlands: new temperature dataset and modelling. Netherlands Journal of Geosciences-Geologie en Mijnbouw 91, 491-515.

Breunese, J.N., van Thienen-Visser, K., 2014. Effecten van verschillende productiescenario's op de verdeling van den compactie in het Groningen veld in de periode 2014 tot en met 2016 R10427, 1-29.

Carlson, M.R., 2003. Practical reservoir simulation: using, assessing, and developing results. PennWell Books.

Croucher, A., 2014. PyTOUGH user's guide 1.4.0, 1-99.

de Jager, J., Geluk, M.C., 2007. Petroleum Geology, in: Wong, T.E., Batjes, D.A.J., de Jager, J. (Eds.), Geology of the Netherlands. Royal Netherlands Academy of Arts and Sciences, Amsterdam, Netherlands, pp. 241-264.

Florian Wellmann, J., Croucher, A., Regenauer-Lieb, K., 2012. Python scripting libraries for subsurface fluid and heat flow simulations with TOUGH2 and SHEMAT. Computers & Geosciences 43, 197-206.

Francke, H., Thorade, M., 2010. Density and viscosity of brine: An overview from a process engineers perspective. Chemie der Erde - Geochemistry 70, Supplement 3, 23-32.

Frick, S., Regenspurg, S., Kranz, S., Milsch, H., Saadat, A., Francke, H., Brandt, W., Huenges, E., 2011. Geochemical and Process Engineering Challenges for Geothermal Power Generation. Chemie Ingenieur Technik 83, 2093-2104.

Grötsch, J., Sluijk, A., van Ojik, K., de Keijzer, M., Graaf, J., Steenbrink, J., 2011. The Groningen gas field: fifty years of exploration and gas production from a Permian

dryland reservoir, in: Grötsch, J., Gaupp, R. (Eds.), The Permian Rotliegend of the Netherlands. SEPM (Society for Sedimentary Geology), Oklahoma, USA, pp. 11-33.

Henares, S., Bloemsma, M.R., Donselaar, M.E., Mijnlieff, H.F., Redjosentono, A.E., Veldkamp, H.G., Weltje, G.J., 2014. The role of detrital anhydrite in diagenesis of aeolian sandstones (Upper Rotliegend, The Netherlands): Implications for reservoir-quality prediction. Sedimentary Geology 314, 60-74.

Legarth, B., Huenges, E., Zimmermann, G., 2005. Hydraulic fracturing in a sedimentary geothermal reservoir: Results and implications. International Journal of Rock Mechanics and Mining Sciences 42, 1028-1041.

Ligtenberg, H., Okkerman, J., de Keijzer, M., 2011. Fractures in the Dutch Rotliegend - An overview, in: Grötsch, J., Gaupp, R. (Eds.), The Permian Rotliegend of the Netherlands. SEPM (Society for Sedimentary Geology), Oklahoma, USA, pp. 229-244.

Mottaghy, D., Pechnig, R., Vogt, C., 2011. The geothermal project Den Haag: 3D numerical models for temperature prediction and reservoir simulation. Geothermics 40, 199-210.

Rockware, 2014. PetraSim.

Saeid, S., Al-Khoury, R., Nick, H.M., Hicks, M.A., 2015. A prototype design model for deep low-enthalpy hydrothermal systems. Renewable Energy 77, 408-422.

Schlumberger, 2012. Petrel 2012 Geology and modelling 12-IS-0333.

Tanikawa, W., Shimamoto, T., 2009. Comparison of Klinkenberg-corrected gas permeability and water permeability in sedimentary rocks. International Journal of Rock Mechanics and Mining Sciences 46, 229-238.

van Heekeren, V., Bakema, G., 2015. The Netherlands Country Update on Geothermal Energy, 1-6.

Van Hulten, F.F.N., 2010. Geological factors effecting compartmentalization of Rotliegend gas fields in the Netherlands. Geological Society, London, Special Publications 347, 301-315.

van Leeuwen, L., Böker, U., van de Weerd, A., 2014. Geothermal Energy in Groningen Geological investigation (Groot Geologisch Onderzoek Groningen) G1111, 1-99.

van Wees, J.D., Kronimus, A., van Putten, M., Pluymaekers, M.P.D., Mijnlieff, H., van Hooff, P., Obdam, A., Kramers, L., 2012. Geothermal aquifer performance assessment for direct heat production—Methodology and application to Rotliegend aquifers. Netherlands Journal of Geosciences-Geologie en Mijnbouw 91, 651.

Van Wees, J.D., Buijze, L., Van Thienen-Visser, K., Nepveu, M., Wassing, B.B.T., Orlic, B., Fokker, P.A., 2014. Geomechanics response and induced seismicity during gas field depletion in the Netherlands. Geothermics 52, 206-219.

Verweij, H., Simmelink, E., Underschultz, J., 2011. Pressure and fluid flow systems in the Permian Rotliegend in the Netherlands onshore and offshore, in: Grötsch, J., Gaupp, R. (Eds.), The Permian Rotliegend of the Netherlands. SEPM (Society for Sedimentary Geology), Oklahoma, USA, pp. 247-263.

Vogt, C., Mottaghy, D., Wolf, A., Rath, V., Pechnig, R., Clauser, C., 2010. Reducing temperature uncertainties by stochastic geothermal reservoir modelling. Geophysical Journal International 181, 321-333.

Vogt, C., Iwanowski-Strahser, K., Marquart, G., Arnold, J., Mottaghy, D., Pechnig, R., Gnjezda, D., Clauser, C., 2013. Modeling contribution to risk assessment of thermal production power for geothermal reservoirs. Renewable Energy 53, 230-241.

Zimmermann, G., Reinicke, A., 2010. Hydraulic stimulation of a deep sandstone reservoir to develop an Enhanced Geothermal System: Laboratory and field experiments. Geothermics 39, 70-77.

Acknowledgements

This research was supported by the research grant Flexiheat (Ministerie van Economische Zaken, Landbouw en Innovatie). The authors would further like to acknowledge Nederlandse Aardolie Maatschappij BV (NAM, a Shell operated 50-50 joint venture with ExxonMobil) for providing the 3D seismic data and Schlumberger for the academic Petrel license.